Laser and Particle Beams (2014), *32*, 509–515.

doi:10.1017/S0263034614000342

Enhanced laser ion acceleration with a multi-layer foam target assembly

E. YAZDANI,[1] R. SADIGHI-BONABI,[2] H. AFARIDEH,[1] J. YAZDANPANAH,[2] AND H. HORA[3]

[1]Department of Energy Engineering and Physics, Amirkabir University of Technology, Tehran, Iran
[2]Department of Physics, Sharif University of Technology, Tehran, Iran
[3]Department of Theoretical Physics, University of New South Wales, Sydney, Australia

(Received 16 March 2014; Accepted 18 June 2014)

Abstract

Interaction of a linearly polarized Gaussian laser pulse (at relativistic intensity of 2.0×10^{20} Wcm^{-2}) with a multi-layer foam (as a near critical density target) attached to a solid layer is investigated by using two-dimensional particle-in-cell simulation. It is found that electrons with longitudinal momentum exceeding the free electrons limit of $m_e c a_0^2/2$ so-called super-hot electrons can be produced when the direct laser acceleration regime is fulfilled and benefited from self-focusing inside of the subcritical plasma. These electrons penetrate easily through the target and can enhance greatly the sheath field at the rear, resulting in a significant increase in the maximum energy of protons in target normal sheath acceleration regime. The results indicate that the maximum proton energy is enhanced by 2.7 times via using an assembled target arrangement compared to a bare solid target. Furthermore, by demonstration of this assembly, the maximum proton energy is improved beyond the optimum amount achieved by a two-layer target proposed by Sgattoni *et al*. (2012).

Keywords: Critical density; Hot electron; Laser pulse; Simulation

INTRODUCTION

Since the invention of chirped pulse amplification, the construction of compact ultra-intense and ultra-short laser pulses has become feasible. Propagation of such laser pulses has been investigated in various plasma conditions (Wang *et al*., 2011; Sadighi-Bonabi *et al*., 2011) resulted in generation of mono-energetic electrons (Faure *et al*., 2004; Sadighi-Bonabi *et al*., 2010; Yazdanpanah *et al*., 2014) protons and ions (Hegelich *et al*., 2006; Yazdani *et al*., 2009; Sadighi-Bonabi *et al*., 2010; Hora *et al*., 2012) and X-rays (Nikzad *et al*., 2012; Shirozhen *et al*., 2014). Laser based ion acceleration is highly attractive due to its potential applications, including fast ignition (Roth *et al*., 2001), proton radiography (Borghesi *et al*., 2006), and so on. One of the critical issues for the development of the laser-driven ion source is enhancement of the ion energy, which is a fundamental requirement of various applications including medical purposes (Malka *et al*., 2004; Borghesi *et al*., 2009).

Various mechanisms of laser-ion acceleration have been proposed to explain the acceleration methods including target normal sheath acceleration (TNSA) (Hattchett *et al*., 2000), shock acceleration (Henig *et al*., 2009), Coulomb explosion (Bulanov *et al*., 2008), radiation pressure acceleration or skin-layer ponderomotive acceleration (Esirkepov *et al*., 2004; Yazdani *et al*., 2009), and laser break-out afterburner acceleration (Jung *et al*., 2013). At present accessible laser intensities, only indirect ion acceleration is possible. In the TNSA model, ions are accelerated on the rear surface of a thin target by a quasi-electrostatic field created by the fast electrons propagating from the target front side. In this regime, proton beams with energies up to 65 MeV have been reported (Gaillard *et al*., 2011).

Many proposals have been suggested to improve the laser absorption by modification in laser and target parameters such as pulse contrast, laser beam shaping, polarization (Daido *et al*., 2012), mass limited target (Limpouch *et al*., 2008), micro-structured surface target for the ion energy enhancement (Margarone *et al*., 2012; Ceccotti *et al*.

Address correspondence and reprint requests to: R. Sadighi-Bonabi, Department of Physics, Sharif University of Technology, P.O. Box 11365-9567, Tehran, Iran. E-mail: sadighi@sharif.ir; or Hossein-Afarideh, Department of Energy Engineering and Physics, Amirkabir University of Technology, P.O. Box 15875-4413, Tehran, Iran. E-mail: hafarideh@aut.ac.ir

2013), and decreasing of target thickness to boost the electron recirculation (Mackinnon *et al.*, 2002). Furthermore, particular attention has been paid to near critical target for ion acceleration due to advantages of higher energy coupling from laser to electrons (Bulanov *et al.*, 2010; Willingale *et al.*, 2011). The interaction of laser beam with electrons is greatly influenced by target density. In the solid target, the interaction takes place on the surface. On the other hand, the laser beam is able to go through the target if the density is sub-critical, as in the case of a gas jet. Such a low density target introduces an extended interaction length to the laser and enables a higher energy gain for the electrons. Creating a near-critical density plasma for wavelength around 1 μm ($n_c = 10^{21}$ cm^{-3}) with sharp density gradient is challenging experimentally. Solid targets have a very high plasma density in a range of 10^{23}–10^{24} cm^{-3} in ionized condition. The critical density takes places somewhere within the expanding plasma, but it would not be in a sharp boundary or in a region with constant near-critical density over a significant distance. Supersonic gas jet targets are useful for producing plasma densities in the range of 10^{18}–10^{20} cm^{-3}, but not much higher (Sylla *et al.*, 2013). Although this is a useful method to produce critical densities for far infra-red wavelengths such as in carbon dioxide lasers, it is far below the quantities needed for near infrared or visible ranges, for example, in Nd:YAG lasers. To produce near-critical density plasma with these lasers, low density foam targets are excellent choices where the produced long uniform initial plasma density can be determined by the initial target size. A foam material is defined by reduction of mass density down to 10^{-3} of solid target density and it can only be a few mg/cc. More recently, a foam material with a thickness of 5–80 micron and density of 1–1000 mg/cc has been manufactured (Zani *et al.*, 2013). This can provide an ideal near-critical density for high contrast lasers such as Ti:sapphire laser.

In a three layer target configuration (with one layer foam) proposed by Nakamura *et al.* (2010) and Sgattoni *et al.* (2012), it was found that the presence of near-critical plasma increases the conversion efficiency, significantly, and leads to enhancement of proton acceleration. This important result led to the motivation to study multi-layer foams with near critical densities. In this work, interaction of short laser pulse with a new target assembly composed of three foam layers with uprising densities in front of Al target is presented. The accelerated electron beams during interaction with near critical density layers have been investigated and categorized to explain the proton energy enhancement in comparison to bare solid target. It is noticed that in three layer target arrangement the relativistic self-focusing is increased considerably by using a foam target. However, it is further improved in multi-layer assembled target and the spot size is reduced from 5 μm to 1.7 μm. Furthermore, a considerable increasing on the accelerated proton energy is achieved. This is explained in more detail.

SIMULATION PARAMETERS

The simulations are performed by using the parallel PIC code extreme laser-matter interaction simulator (ELMIS; http://www.ipfran.ru/english/structure/lab334/simlight.html; Gonoskov *et al.*, 2009). In the relativistic code of ELMIS, Maxwell's equations are solved by using a parallel fast Fourier transform technique. The target consists of foam layers with an electron density from $0.3n_c$ to $1.2n_c$, located in $64 < x < 85$ and $-8 < y < 8$, where n_c is critical density, x and y are in micrometer; with thickness of 7 μm for each layer, a 0.5 μm Al solid layer with electron density of $45n_c$ and a 60 nm contaminant layer of protons and electrons with a density of $8n_c$ as the last layer in the target design.

In our simulations, a linearly polarized laser pulse with duration of $\tau_L = 80$ fs (FWHM, Gaussian profile) and wavelength of $\lambda_L = 1$ μm is focused into spot of 5 μm on the target surface. The maximum laser intensity used in this simulation is 2×10^{20} Wcm^{-2}. The size of simulation box is 128 μm × 32 μm (8192 × 2048 cells) with absorbing boundaries for the fields and particles. The initial plasma temperature is set to 0.3 keV, and the cell size is 15.625 nm, which is four times of the Debye length for the considered plasma. The time steps are set to $(2\pi/\omega_p)/16 \approx 3.0 \times 10^{-17}$ s, where $\omega_p = (4\pi e 45 n_c/m_e)^{1/2}$ is the plasma frequency. Structure of the multi-layer target assembly is shown in Figure 1.

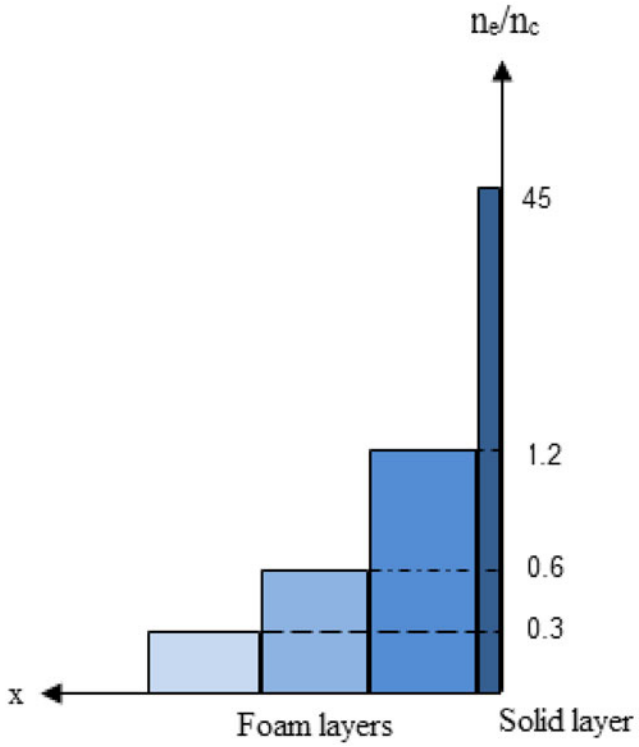

Fig. 1. Structure of the multi-layer target assembly.

https://doi.org/10.1017/S0263034614000342 Published online by Cambridge University Press

RESULTS AND DISCUSSION

The incident laser pulse at relativistic intensity of 2×10^{20} Wcm^{-2} is self-focused as it propagates in the foam layer, as it is shown in Figure 2 at $t = 49\tau$, where, τ is the time of one laser cycle ($\tau = \lambda c$ is the speed of light, for wavelength $\lambda = 1$ μm; τ comes out to be 3.33 fs). A laser pulse experiences relativistic self-focusing in the condition when the laser power exceeds the critical power of $P_{cr} \approx 17(\omega_0/\omega_p)^2$ GW, where ω_0 and ω_p are plasma and laser frequencies, respectively (Hora, 1973; 1975). For the foam layer with average density of about $0.3n_c$ the critical power becomes $P_{cr} \sim 1.8\times10^{11}$ W; this is related to the laser intensity of $I = 7.2\times10^{17}$ W/cm^2 with 5 μm spot radius. Figure 2 shows the laser envelope, E_y, along the laser propagation axis. It can be realized that the laser pulse is self-focused rapidly in the foam layers in a tight focal spot with the diameter of 1.7 μm before interaction with the solid layer. It should be mentioned that the foam thickness is selected in a way to provide the maximum focusing along it. Therefore, there is a careful matching between the optimum self-focusing and foam thickness at the defined densities.

Two typical groups of electrons are recognized from the simulation, which are shown in Figure 3. The first group of the electrons with densities much higher than the background electrons is created by ponderomotive force of the focused pulse that expels the local plasma electrons, leads to an ion channel formation behind it. The second group of electrons experiences the direct laser acceleration (DLA) via betatron resonance which was proposed by Pukhov *et al.* (1999). It should be noticed that high energy electrons are produced via several mechanisms in underdense plasma, such as: DLA, stochastic heating, LWFA, and nonlinear self-focusing. In this study, the contribution of LWFA is ignored due to much larger laser pulse duration in comparison to the plasma wavelength and limitation of the acceleration distance (Geddes *et al.*, 2004). Relativistic self-focusing and DLA regime explained by transverse betatron oscillation of energetic electrons are the dominant approaches in the present simulation. Under these circumstances, when the laser frequency is close to the betatron frequency of electrons, an efficient energy exchange is possible.

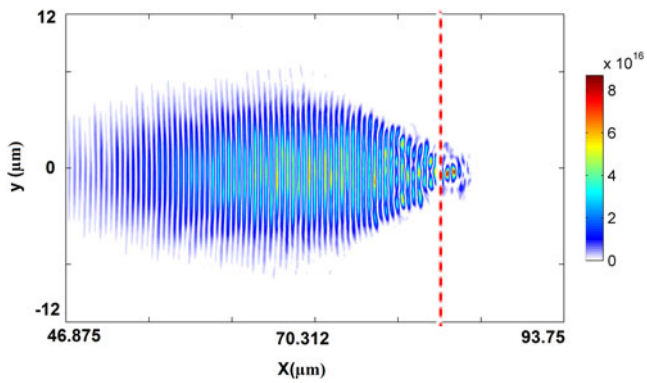

Fig. 2. Indicates the laser envelope E_y along the laser propagation axis at $t = 49\tau$ for multi-layer target. The laser intensity is 2×10^{20} Wcm^{-2} with 80 fs laser pulse duration. The initial laser spot size is 5 μm.

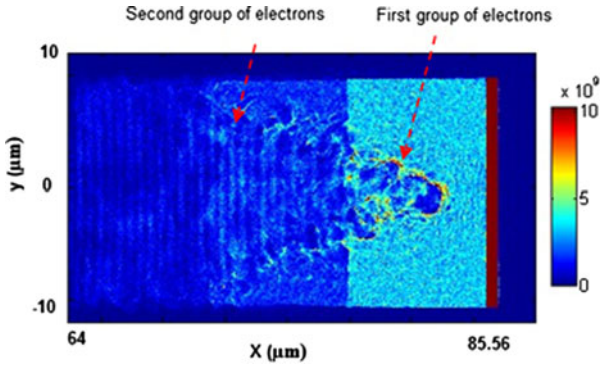

Fig. 3. Electron density map at $t = 49\tau$ for multi-layer target.

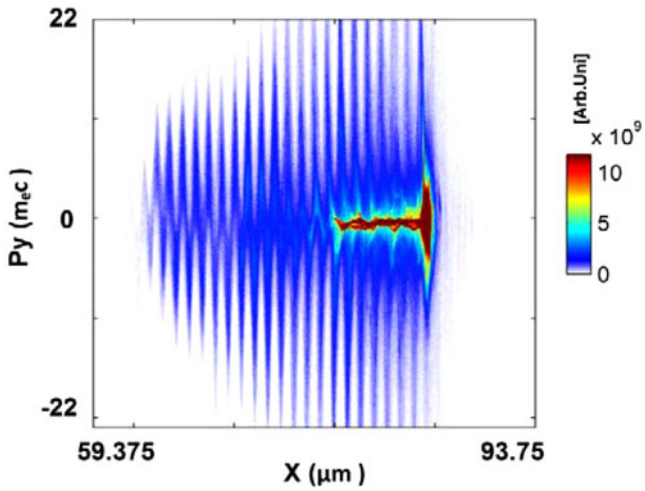

Fig. 4. Transverse momentum, p_y, of the electrons for target with multi-layer foam layer at $t = 65\tau$ is indicated.

Figure 4 illustrates that the transverse momentum of the electrons increases with the laser penetration distance and can reach to a maximum of about $22m_ec$. This is about two times higher than the amount given by $p_y = a_0m_ec$, ($12\ m_ec$ is the amount of the relativistic electron in plane electromagnetic wave in vacuum) (Yu *et al.*, 2000). The transverse momentum of the electrons, p_y, is converted into longitudinal momentum, P_x, via $V\times B$ interaction; for the fast electrons P_x can reach to $134m_ec$, as it is observed in Figure 5. This is about 80% more than the amount achieved by $P_x = a_0^2m_ec/2 = 72m_ec$ in vacuum (Yu *et al.*, 2000; Gahn *et al.*, 1999). These electrons with momentum exceeding $a_0^2m_ec/2$ could be called super-hot electrons due to their much higher temperature compared to the ponderomotive scaling of electrons defined by Wilks *et al.* (1992). The oscillation frequency of the longitudinal momentum is twice that of

https://doi.org/10.1017/S0263034614000342 Published online by Cambridge University Press

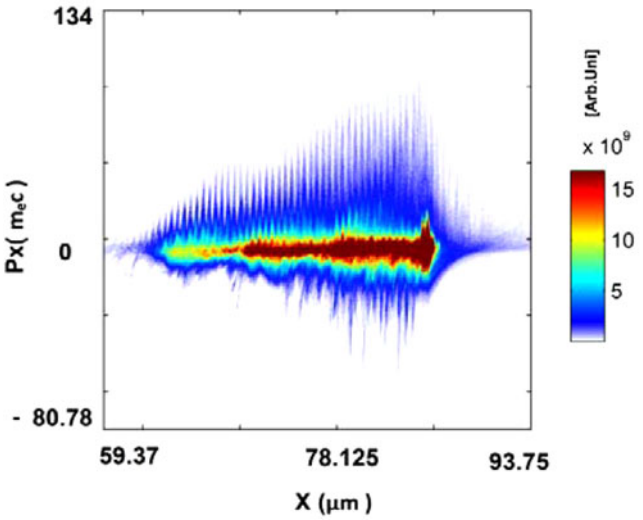

Fig. 5. Longitudinal momentum, px, of the electrons for target with multi-layer foam at $t = 65\tau$ is presented.

the transverse momentum (ω_0). The reason of ion energy increment is obviously due to the fact that the laser wavelength λ_0 has a relativistic increase $\lambda = \lambda_0/n(I)$ (Hora, 1975). The nonlinear optical properties of plasma due to the relativistic electron motion in an intense laser field are of fundamental importance in generation of laser driven sources of particles.

Three types of cold, hot, and super-hot electrons are generated in interaction of laser with the multi-layer target assembly. As mentioned before, TNSA is an ion acceleration regime by thermal electrons (Snavely *et al.*, 2000) and it is valid for solid targets with a wide thickness range: hundreds of nanometers to a few micrometers. The thermal electron temperature obtained by the relativistic oscillation energy so called hot electrons (Wilks *et al.*, 1992):

$$T_e = m_e c^2[(1 + a_0^2)^{1/2} - 1], \quad (1)$$

where m_e is the electron mass, c is the speed of light, and a_0 is the normalized laser amplitude. The electrons with temperatures lower than T_e of Eq. (1) are called cold, and those with temperature larger than T_e are named super-hot electrons, where the latter are produced by interaction of an intense laser with a solid target covered by foam layers.

The electron energy spectrum at 71τ is shown in Figures 6a and 6b. It demonstrates an exponential dependence of dN/dE to $-1/T_e$, from $dN/dE \propto \exp(-E/T_e)$, where E is electron energy and T_e refers to effective temperature. In Figure 6a for the multi-layer foam target, in the selected range of E from 10 to 50 MeV, T_e is 7.9 MeV, which is 45% more than the estimated amount by the ponderomotive or hot electron scaling, Eq. (1). In Figure 6b for the bare solid target, the effective temperature in the selected range of E from 5 to 18 MeV, T_e is 2.2 MeV. It should be emphasized that with introducing a near critical density layer, not only the domain of hot electrons is increased, but also much higher

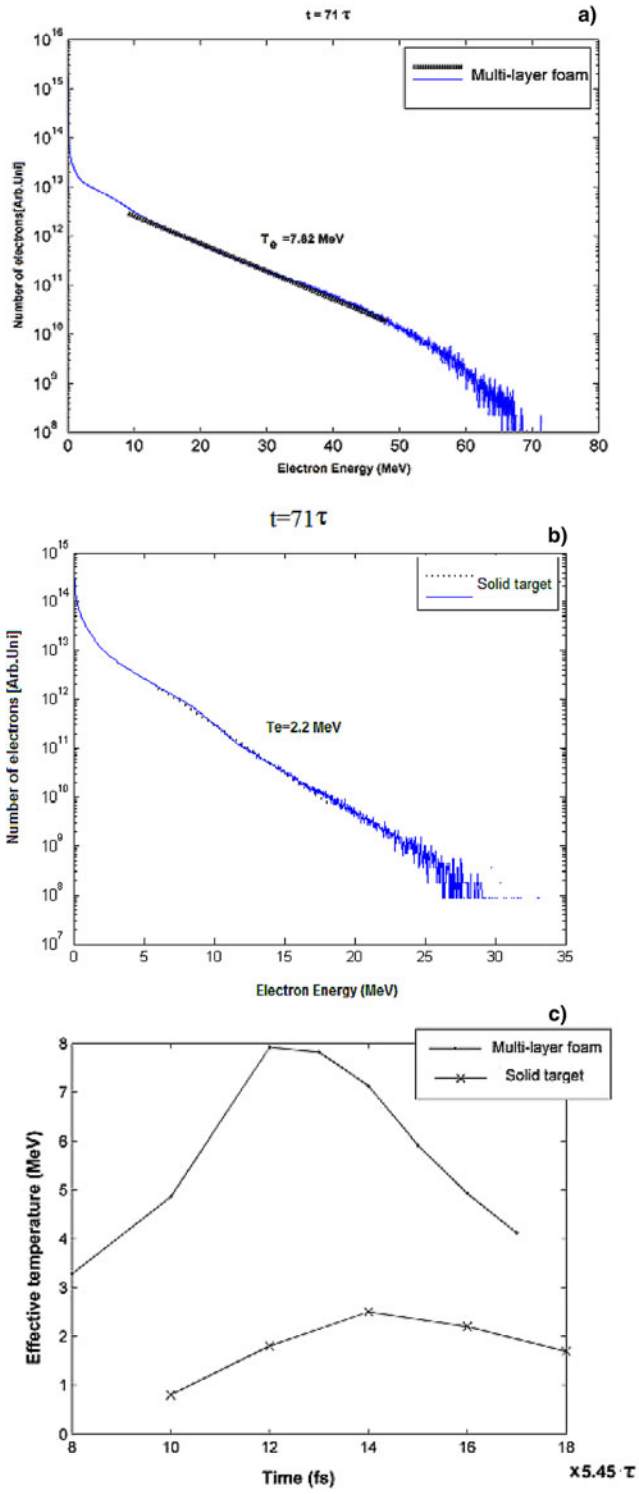

Fig. 6. The energy spectrum of the electrons at $t = 71\tau$ for case of multi-layer foam (**a**) and for bare solid target (**b**). The evolution of the energetic electrons temperature for different target compositions (**c**) is shown.

energy cut-off is realized due to dominant regime of DLA. Figure 6c presents the evolution of effective temperature for the energetic electrons with an estimation of the maximum temperature for different target configurations. For

https://doi.org/10.1017/S0263034614000342 Published online by Cambridge University Press

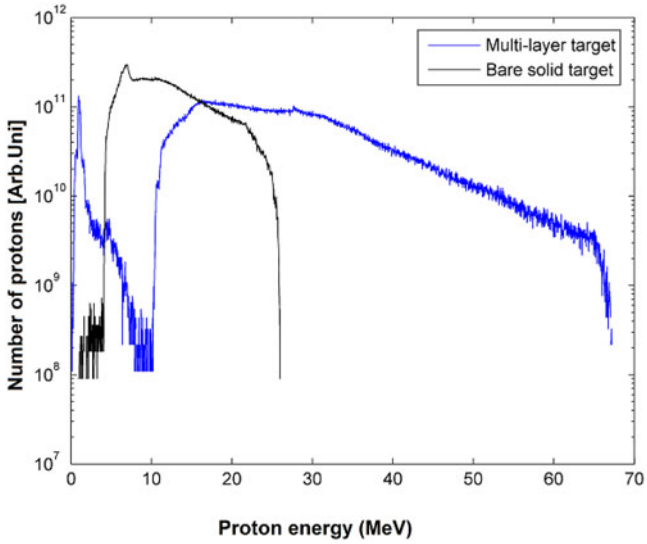

Fig. 7. The energy spectrum of protons at $t = 109\tau$ for bare solid (black) and multi-layer foam attached to the solid target (blue) are presented.

the attached foam to the solid foil, T_e increases almost linearly versus time to a maximum of about 8 MeV at $t \sim 71\tau$. The comparison of Figures 6a and 6b represents that by increasing the interaction time, decreasing of T_e in the target with foam is larger and faster than the solid target due to the status of energy transfer from electrons to ions. This is observed more clearly in Figure 6c.

Figure 7 shows the proton energy spectrum for different target compositions. It is noticed that the proton cut-off energy for the multi-layer foam configuration has the highest amount; it is about 2.7 times of the bare solid target. It can also be seen that the proton energy spectrum has a smooth cut-off and the number of high energy protons is increased for this target, which is demanding in some applications.

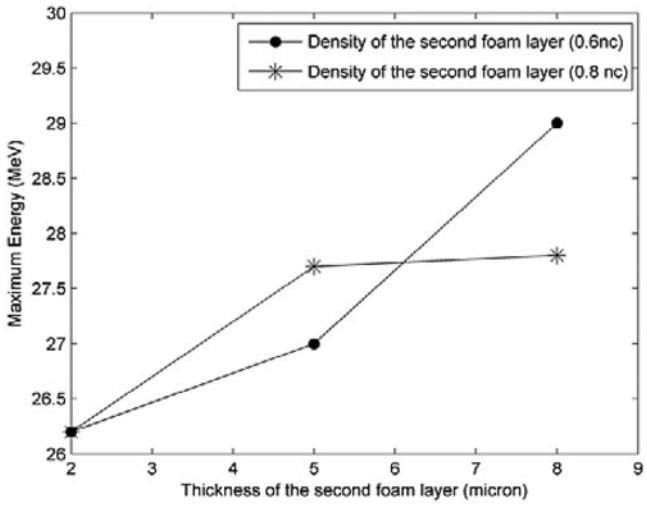

Fig. 8. Shows the maximum proton energy versus different density and thickness of the second foam layer.

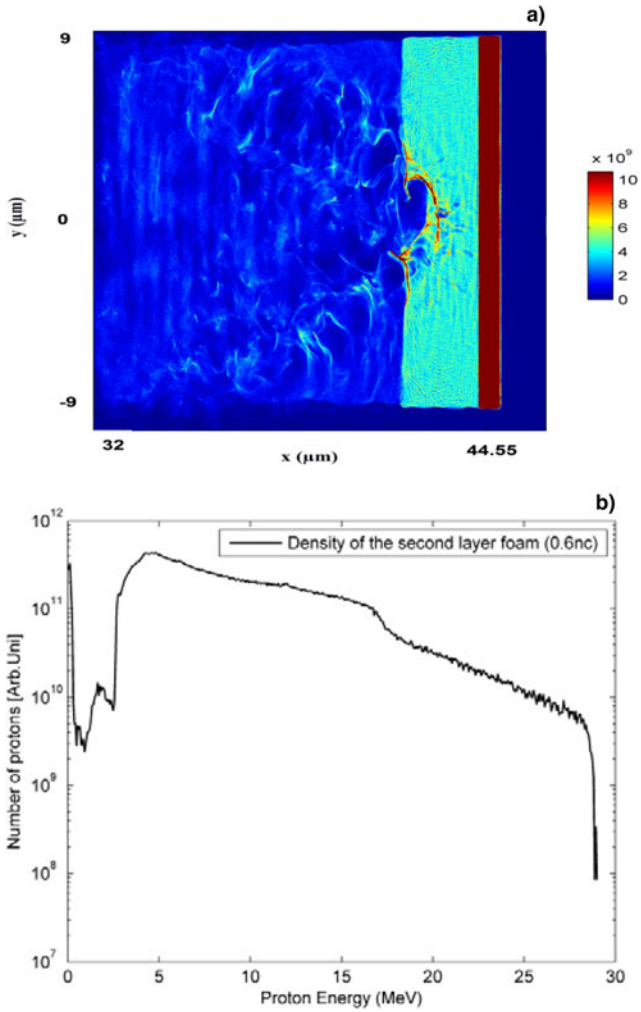

Fig. 9. The electron density map at 27τ (**a**) and the proton energy spectrum (**b**) are presented.

When the laser pulse propagates through the foam layer, the laser penetration length and self-focusing are increased, resulting in the enhancement of interaction intensity to higher values. In low density foam, by increasing of the laser propagation through the plasma, laser energy absorption by electrons is decreased. But for foam with slightly higher density, laser energy absorption by electrons due to the volume interaction is dominated. The simultaneous effects of these factors result in an optimum condition for effective energy transformation to the electrons. The optimum amounts of density and thickness for the foam layer has been determined in Sgattoni *et al.* (2012). In this study, it is shown that by adding an extra foam layer with slightly lower density to the optimum condition of the Sgattoni's work, the laser self-focusing is stimulated and therefore further energy absorption and heating experienced by ions and electrons. The new simulations are carried out by using the optimum parameters for the first foam layer with 2 μm thickness and $2n_c$ density, and the second foam layer with series of data: $0.6n_c$–$0.8n_c$ for density and thickness of 0, 5, and 8 μm

https://doi.org/10.1017/S0263034614000342 Published online by Cambridge University Press

and the same laser parameters of Sgattoni's work (Sgattoni *et al*., 2012) are employed. Figure 8 shows that in this new arrangement, furtherer improvement is achieved in maximum proton energy and confirms the priority of a multi-layer arrangement in comparison using only one foam target. For more clarification, the electron density map at 27τ Figure 9a. and the proton energy spectrum for multi-layer target which contain two foam layers with 8 μm and 2 μm thickness and density of $0.6n_c$ and $2n_c$, respectively, in Figure 9b are indicated.

CONCLUSION

In this work, proton acceleration from interaction of ultra-intense linearly polarized laser pulse with a multi-layer assembled target is studied by using two-dimensional particle-in-cell simulation. In this assembled target, electron heating is improved under the action of DLA and laser pulse self-focusing which leads to stronger electrostatic field generation at the target back for relatively long time. In this arrangement, the maximum proton energy is increased up to 2.7 times of the amount produced without sub-critical density plasma. The amount of the accelerated protons with higher energy is also increased, considerably, and the cut-off energy is obtained following a smooth reduction of protons number. Furthermore, it is noticed that with the mentioned arrangement, additional improvement is achieved in maximum proton energy and confirms the priority of a multi-layer arrangement in comparison using only one foam target. Based on the achieved outcomes and due to the possible technology for fabrication of new foam targets, it is suggested to do further investigation on electron heating via interaction of ultra-intense laser pulses with these targets at the critical density and even at the related effective critical density, which are not feasible at the common solid targets.

ACKNOWLEDGEMENT

The authors would like to acknowledge Prof. C. G. Wahlstrom, Prof. M. Marklund, Dr. A. V. Korzhimanov, Dr. O. Lundh and Dr. L. Nikzad for their supports. Special thanks to Dr. A. Gonoskov for his PIC code and useful comments.

REFERENCES

Borghesi, M., Fuchs, J., Bulanov, S.V., Mackinnon, A.J., Patel, P.K. & Roth, M. (2006). Fast ion generation by high-intensity laser irradiation of solid targets and applications. *Fusion Sci. Technol.* **49**, 412.

Borghesi, M., Toncian, T., Fuchs, J., Cecchetti, C.A., Romagnani, L., Kar, S., Quinn, K., Ramakrishna, B., Wilson, P.A., Antici, P., Audebert, P., Brambrink, E., Pipahl, A., Jung, R., Amin, M., Willi, O., Larke, R.J., Notley, M., Mora, P., Grismayer, T., D'humières, E. & Sentoku, Y. (2009). Laser-driven proton acceleration and applications: Recent results. *EPJST* **175**,105.

Bulanov, S.S., Brantov, A., Bychenkov, V.Yu., Chvykov, V. , Kalinchenko, G., Matsuoka, T., Rousseau, P., Reed, S., Yanovsky, V., Litzenberg, D.W., Krushelnick, K. & Maksimchuk, A. (2008). Accelerating monoenergetic protons from ultrathin foils by flat-top laser pulses in the directed-Coulomb-explosion regime. *Phys. Rev. E* **78**, 026412.

Bulanov, S.S., Bychenkov, V.Y, Chvykov, V., Kalinchenko, G., Litzenberg, D.W., Matsuoka, T., Thomas, A.G.R., Willingale, L., Yanovsky, V., Krushelnick, K. & Maksimchuk, A. (2010). Generation of GeV protons from 1 PW laser interaction with near critical density targets. *Phys. Plasmas* **17**, 0431052010.

Ceccotti, T., Floquet, V., Sgattoni, A., Bigongiari, A., Raynaud, M., Riconda, C., Heron, A., Baffigi, F., Labate, L., Gizzi, L.A., Vassura, L., Fuchs, J., Passoni, M., Kveton, M., Novotny, F., Possolt, M., Prokupek, J., Proska, J., Psikal, J., Stolcova, L., Velyhan, A., Bougeard, M., D'oliveira, P., Tcherbakoff, O., Reau, F., Martin, P. & Macchi, A. (2013). Evidence of resonant surface-wave excitation in the relativistic regime through measurements of proton acceleration from grating targets. *Phys. Rev. Lett.* **111**, 185001.

Daido, H., Nishiuchi, M. & Pirozhkov, A.S. (2012). Review of laser-driven ion sources and their applications. *Rep. Prog. Phys.* **75**, 056401.

Esirkepov, T., Borghesi, M., Bulanov, S.V., Mourou, G. & Tajima, T. (2004). Highly efficient relativistic-ion generation in the laser-piston regime. *Phys. Rev. Lett.* **92**, 175003.

Faure, J., Glinec, Y., Pukhov, A., Kiselev, S., Gordienko, S., Lefebvre, E., Rousseau, J.-P., Burgy, F. & Malka, V. (2004). A laser–plasma accelerator producing monoenergetic electron beams. *Nature* **431**, 541–544.

Gahn, C., Tsakiris, G.D., Pukhov, A., Meyer-Ter-Vehn, J., Pretzler, G., Thirolf, P., Habs, D. & Witte, K.J. (1999). Multi-MeV electron beam generation by direct laser acceleration in high-density plasma channels. *Phys. Rev. Lett.* **83**, 4772.

Gaillard, S.A., Kluge, T., Flippo, K.A., Bussmann, M., Gall, B., Lockard, T., Geissel, M. Offermann, D.T., Schollmeier, M., Sentoku, Y. & Cowan, T.E. (2011). Increased laser-accelerated proton energies via direct laser-light-pressure acceleration of electrons in micro-cone targets. *Phys. Plasmas* **18**, 056710.

Geddes, C.G.R., Toth, CS., Tilborg, J.Van., Esarey, E., Schroeder, C.B., Bruhwiler, D., Nieter, C., Cary, J. & Leemans, W.P. (2004). High-quality electron beams from a laser wake field accelerator using plasma-channel guiding. *Nature* **431**, 538–541.

Gonoskov, A.A., Korzhimanov, A.V., Eremin, V.I., Kim, A.V. & Sergeev, A.M. (2009). Multicascade proton acceleration by a superintense laser pulse in the regime of relativistically induced slab transparency. *Phys. Rev. Lett.* **102**, 184801.

Hatchett, S.P., Brown, C.G., Cowan, T.E., Henry, E.A., Johnson, J.S., Key, M.H., Koch, J.A., Langdon, A.B., Lasinski, B.F., Lee, R.W., Mackinnon, A.J., Pennington, D.M., Perry, M.D., Phillips, T.W., Roth, M., Sangster, T.C., Singh, M.S., Snavely, R.A., Stoyer, M.A., Wilks, S.C. & Yasuike, K. (2000). Electron, photon, and ion beams from the relativistic interaction of Petawatt laser pulses with solid targets. *Phys. Plasmas* **7**, 2076.

Hegelich, B.M., Albright, B.J., Cobble, J., Flippo, K., Letzring, S., Paffett, M., Ruhl, H., Schreiber, J., Schulze, R.K. & Fernández, J.C. (2006). Laser acceleration of quasi-monoenergetic MeV ion beams. *Nature* **439**, 441–444.

Henig, A., Kiefer, D., Geissler, M., Rykovanov, S.G., Ramis, R., Hörlein, R., Osterhoff, J., Major, Z.S., Veisz, L., Karsch, S., Krausz, F., Habs, D. & Schreiber, J. (2009). Laser-driven

https://doi.org/10.1017/S0263034614000342 Published online by Cambridge University Press

shock acceleration of ion beams from spherical mass-limited targets. *Phys. Rev. Lett.* **102**, 095002.

Hora, H., Sadighi-Bonabi, R., Yazdani, E., Afarideh, H., Nafari, F. & Ghorannevis, M. (2012). Effect of quantum correction on the acceleration and delayed heating of plasma blocks. *Phys. Rev. E* **85**, 036404.

Hora, H. (1975). Theory of relativistic self-focusing of laser radiation in plasmas. *J. Opt. Soc. Am.* **65**, 882.

Hora, H. (1973). Relativistic oscillation of charged particles in laser fields and pair production. *Nature Phys. Sci.* **243**, 34.

Jung, D., Yin, L., Gautier, D.C., Wu, H.C., Letzring, S., Dromey, B., Shah, R., Palaniyappan, S., Shimada, T., Johnson, R.P., Schreiber, J., Habs, D., Fernández, J.C., Hegelich, B.M. & Albright, B.J. (2013). Laser-driven 1 GeV carbon ions from preheated diamond targets in the break-out afterburner regime. *Phys. Plasmas* **20**, 083103.

Limpouch, J., Psikal, J., Andreev, A.A., Platonov, K.Yu. & Kawata, S. (2008). Enhanced laser ion acceleration from mass-limited targets. *Laser Part. Beams* **26**, 225.

Mackinnon, A.J., Sentoku, Y., Patel, P.K., Price, D.W., Hatchett, S., Key, M.H., Andersen, C., Snavely, R. & Freeman, R.R. (2002). Enhancement of proton acceleration by hot-electron recirculation in thin foils irradiated by ultraintense laser pulses. *Phys. Rev. Lett.* **88**, 215006.

Malka, V., Fritzler, S., Lefebvre, Erik, D'humieres, E., Ferrand, R., Grillon, G., Albaret, C., Meyroneinc, S., Chambaret, J.P., Antonetti, A. & Hulin, D. (2004). Practicability of proton therapy using compact laser systems. *D. Med. Phys.* **31**, 1587.

Margarone, D., Klimo, O., Kim, I.J., Prokupek, J., Limpouch, J., Jeong, T.M., Mocek, T., Psikal, J., Kim, H.T., Proska, J., Hnam, K., Stolcova, L., Choi, I.W., Lee, S.K., Sung, J.H., Yu, T.J. & Korn, G. (2012). Laser-driven proton acceleration enhancement by nanostructured foils. *Phys. Rev. Lett.* **109**, 234801.

Nakamura, T., Tampo, M., Kodama, R., Bulanovs, V. & Kando, M. (2010). Interaction of high contrast laser pulse with foam-attached target. *Phys. Plasmas* **17**, 113107.

Nikzad, L., Sadighi-Bonabi, R., Riazi, Z., Mohammadi, M. & Heydarian, F. (2012). Simulation of enhanced characteristic x rays from a 40-MeV electron beam laser accelerated in plasma. *Phys. Rev. ST Accel. Beams* **15**, 021301.

Pukhov, A., Sheng, Z.-M. & Meyer-Ter-Vehn, T. (1999). Particle acceleration in relativistic laser channels. *J. Phys. Plasmas* **6**, 2847.

Roth, M., Cowan, T.E., Key, M.H., Hatchett, S.P., Brown, C., Fountain, W., Johnson, J., Pennington, D.M., Snavely, R.A., Wilks, S.C., Yasuike, K., Ruhl, H., Pegoraro, F., Bulanov, S.V., Campbell, E.M., Perry, M.D. & Powell, H. (2001). Fast ignition by intense laser-accelerated proton beams. *Phys. Rev. Lett.* **86**, 436.

Sadighi-Bonabi, R. & Moshkelgosha, M. (2011). Self-focusing up to the incident laser wavelength by an appropriate density ramp. *Laser Part. Beams* **29**, 453.

Sadighi-Bonabi, R. & Rahmatollahpur, S.H. (2010). Potential and energy of the monoenergetic electrons in an alternative ellipsoid bubble model. *Phy. Rev. A.* **81**, 023408.

Sadighi-Bonabi, R., Hora, H., Riazi, Z., Yazdani, E. & Sadighi, S.K. (2010). Generation of plasma blocks accelerated by nonlinear forces from ultraviolet KrF laser pulses for fast ignition. *Laser Part. Beams* **28**, 101.

Sgattoni, A., Londrillo, P., Macchi, A. & Passoni, M. (2012). Laser ion acceleration using a solid target coupled with a low-density layer. *Phys. Rev. E* **85**, 036405.

Shirozhan, M., Moshkelgosha, M. & Sadighi-Bonabi, R. (2014). The effects of circularly polarized laser pulse on generated electron nanobunches in oscillating mirror model. *Laser Part. Beams* (in press).

Snavely, R.A., Key, M.H., Hatchett, S.P., Cowan, T.E., Roth, M., Phillips, T.W., Stoyer, M.A., Henry, E.A., Sangster, T.C., Singh, M.S., Wilks, S.C., Mackinnon, A., Offenberger, A., Pennington, D.M., Yasuike, K., Langdon, A.B., Lasinski, B.F., Johnson, J., Perry, M.D. & Campbell, E.M. (2000). Intense high-energy proton beams from Petawatt-laser irradiation of solids. *Phys. Rev. Lett.* **85**, 2945.

Sylla, F., Flacco, A., Kahaly, S., Veltcheva, M., Lifschitz, A., Malka, V., D'humieres, E., Andriyash, I. & Tikhonchuk, V. (2013). Short intense laser pulse COLLAPSE in near-critical plasma. *Phys. Rev. Lett.* **110**, 085001.

Wang, H.Y., Lin, C., Sheng, Z.M., Liu, B., Zhao, S., Guo, Z.Y., Lu, Y.R., He, X.T., Chen, J.E., & Yan, X.Q. (2011). Laser shaping of a relativistic intense, short gaussian pulse by a plasma lens. *Phys. Rev. Lett.* **107**, 265002.

Wilks, S.C., Kruer, W.L., Tabak, M. & Langdon, A.B. (1992). Absorption of ultra-intense laser pulses. *Phys. Rev. Lett.* **69**, 1383.

Willingale, L., Nilson, P.M., Thomas, A.G.R., Bulanov, S.S., Maksimchuk, A., Nazarov, W., Sangster, T.C., Stoeckl, C. & Krushelnick, K. (2011). High-power, kilojoule laser interactions with near-critical density plasma. *Phys. Plasmas* **18**, 056706.

Yazdani, E., Cang, Y., Sadighi-Bonabi, R., Hora, H. & Osman, F.H. (2009). Layers from initial Rayleigh density profile by directed nonlinear force driven plasma blocks for alternative fast ignition. *Laser Part. Beams* **27**, 149.

Yazdanpanah, J. & Anvari, A. (2014). Effects of initially energetic electrons on relativistic laser-driven electron plasma waves. *Phys. Plasmas* **21**, 023101.

Yu, Wei., Bychenkov, V., Sentoku, Y., Yu, M.Y., Sheng, Z.M. & Mima, K. (2000). Electron acceleration by a short relativistic laser pulse at the front of solid targets. *Phys. Rev. Lett.* **85**, 570.

Zani, A., Dellasega, D., Russo, V. & Passoni, M. (2013). Ultra-low density carbon foams produced by pulsed laser deposition. *Carbon* **56**, 358–365.